Surveys in Geophysics
https://doi.org/10.1007/s10712-021-09669-x

Earth's Rotation: Observations and Relation to Deep Interior

Jérémy Rekier[1] · Benjamin F. Chao[2] · Jianli Chen[3] · Véronique Dehant[1] · Séverine Rosat[4] · Ping Zhu[1]

Received: 19 May 2021 / Accepted: 11 October 2021

Abstract

Observation of the variations in the Earth's rotation at time scales ranging from subdiurnal to multidecadal allows us to learn about its deep interior structure. We review all three types of motion of the Earth's rotation axis: polar motion (PM), length of day variations (ΔLOD) and nutations, with particular attention to how the combination of geodetic, magnetic and gravity observations provides insight into the dynamics of the liquid core, including its interactions with the mantle. Models of the Earth's PM are able to explain most of the observed signal with the exception of the so-called Markowitz wobble. In addition, whereas the quasi-six year oscillations (SYO) observed in both ΔLOD and PM can be explained as the result of Atmosphere, Oceans and Hydrosphere Forcing (AOH) for PM, this is not true for ΔLOD where the subtraction of the AOH only makes the signal more visible. This points to a missing—possibly common—interpretation related to deep interior dynamics, the latter being also the most likely explanation of other oscillations in ΔLOD on interannual timescales. Deep Earth's structure and dynamics also have an impact on the nutations reflected in the values of the Basic Earth Parameters (BEP). We give a brief review of recent works aiming to independently evaluate the BEP and their implications for the study of deep interior dynamics.

Keywords Earth's rotation · Polar motion · Length of day · Nutation · Observations

Article Highlights

- Review of observations of the three components of Earth's rotation using magnetic, gravimetric and geodetic measurements
- Discussion of the implications for the dynamics of the Earth's liquid core
- Perspective on future theoretical and experimental development

---

✉ Jérémy Rekier
jeremy.rekier@observatory.be

[1] Royal Observatory of Belgium, Ringlaan 3, BE-1180 Brussels, Belgium

[2] Academia Sinica, Institute of Earth Sciences, Taipei 115, Taiwan

[3] Center for Space Research, University of Texas, Austin, TX 78759, USA

[4] Université de Strasbourg, CNRS, EOST, IPGS UMR 7516, F-67000 Strasbourg, France

1 Introduction

Variations in the Earth's rotation can all be traced back, ultimately, to transfers of angular momentum, either between the planet and its surrounding—primarily due to the torques exerted by the Sun and Moon—or among the internal layers within the planet itself.

1.1 The Three Components of Earth's Rotation

When talking about variations in rotation, we mean either the changes in the magnitude or direction of the angular velocity vector of the planet or those in the orientation of the planetary figure itself, the two being related by kinematic relations. Changes in the rotation rate result in *variations in the length of day* (ΔLOD). Changes in the rotation axis orientation can be observed as movements of the poles in space. The motion known to astronomers as the *Precession of equinoxes* is a secular motion of that latter type which takes the Earth's pole around the normal to the ecliptic in a period of about 25,700 years. Nutations come in addition to this secular motion manifesting themselves as a series of oscillations of shorter periods about the mean equinox. These are, for the most part, caused by the tidal torques exerted by the Sun and Moon. For historical as well as technical reasons, it is customary to further separate these oscillations in two kinds based on their frequencies. Roughly speaking, one then speaks of (precession–) *nutations* to denote oscillations that have a low frequency as measured from a *Celestial Reference Frame* (CRF), whereas other kind of oscillations is referred to as the *polar motion* (PM). The latter consists mainly of oscillations of subdiurnal frequencies as measured in a *Terrestrial Reference Frame* (TRF) (see Dehant and Mathews (2015) for details).

1.2 Reference Frames

More specifically, when speaking either of nutations or polar motion, we refer to the motion of the *Celestial Intermediate Pole* (CIP) with respect to the *International Celestial Reference Frame* (ICRF) or the *International Terrestrial Reference Frame* (ITRF), respectively. The definition of the CIP was adopted by the *International Astronomical Union* (IAU) in 2000 in order to replace the previous *Celestial Ephemeris Pole* (CEP) and to accommodate significant improvements in the Earth's observation. This led to the formal classification of nutations and PM according to Fig. 1, where nutations are identified as oscillations of the CIP with frequencies $-0.5 \leq \omega \leq 0.5$ (in cycles per sideral day, cpsd)

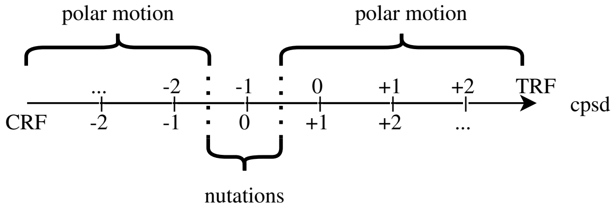

Fig. 1 Conventional definitions of polar motion (PM) and nutations of the CIP. Nutations have frequencies in the interval $-0.5 \leq \omega \leq 0.5$ measured in the Celestial Reference Frame (CRF). PM covers all the remaining corresponding frequencies as they appear in the Terrestrial Reference Frame (TRF). The difference of 1 cycle per sideral day (cpsd) between the two frames corresponds to the diurnal rotation rate of the Earth

as measured from the ICRF, whereas PM are oscillations of the CIP with frequencies in the intervals $-\infty < \omega \leq -0.5$ and $0.5 \leq \omega < \infty$ in the ITRF. As there is a difference of +1 cpsd when going from the ITRF to the ICRF (accounting for the diurnal rotation of the Earth), wobbles of the instantaneous rotation axis with frequencies within the interval −1.5 to −0.5 cpsd (i.e. with periods close to either 2/3 or 2 sideral days corresponding to $\sim$ 15.9h and $\sim$ 47.9h, respectively) are equivalent to nutations. Note that one speaks about wobble instead of PM in this case as PM is a term classically used for the CIP motion in the TRF.

As the Earth's rotation is very close to a steady state, it is customary to write the rotation vector as:

$$\Omega = \Omega_0(\hat{\mathbf{z}} + \mathbf{m}) \,, \tag{1}$$

where we have chosen the Cartesian basis vector, $\hat{\mathbf{z}}$, in the direction of the mean spin-axis. $\Omega_0 = 1$ cpsd denotes the mean angular rate of rotation, and the vector $\mathbf{m}$ is called the planetary *wobble*. This last quantity is typically very small with a magnitude of the order of 10^{-8} to 10^{-6} for the Earth. For this reason, the equations of conservation of angular momentum governing the time evolution of $\mathbf{m}$ can be safely restricted to first order. This effectively decouples the axial component of rotation m^z from the equatorial components m^x and m^y where the Cartesian geographical x coordinate points to the Greenwich Meridian and the y coordinate points to the 90° East longitude. Classically, one then uses the term 'wobble' in relation to the latter two components exclusively. The dynamics of m^z models the modulations in the LOD while m^x and m^y model both PM and nutations expressed in the TRF. Quantitatively, ΔLOD does not exceed a few milliseconds (ms), typical PM is of the order of several hundreds of milliarcseconds (mas) (corresponding to a PM within a square of 20 m side), and the dominant component of nutations (Bradley's nutation of 18.6-year period) has an amplitude of about ±19 arcsec and ±10 arcsec in longitude and obliquity, respectively. The wobble corresponding to nutations is of the order of several milliarcseconds (mas).

1.3 Origins of the Earth's Movement

Broadly speaking, PM is typically associated with variations in the orientation of the rotation axis caused by geophysical processes, i.e. the redistribution of the masses inside the Earth that gets reflected in the inertia tensor. Such redistributions result in both secular and oscillatory variations. On the other hand, nutations are more affected by torques resulting from the tidal forces from external sources (primarily the Moon and Sun). This distinction is, however, a matter of nomenclature. For example, in reality, excitations from outer sources do also cause redistributions of masses inside the Earth (Mathews and Bretagnon 2003). For our purpose, the two types of motions can nevertheless be clearly separated on the basis of observation.

Conventionally in geodesy, studies of PM (including wobble) and nutations assume that the flow inside the core has a uniform vorticity, i.e. it resembles a solid-body rotation around an axis forming a finite angle with the mantle's rotation. It can be shown that the core flow bears little effect on the excitation of PM (see, e.g., Chap. 7 of Bizouard 2020). However, as explained in Sect. 2 the mere presence of the fluid core affects the PM by altering the frequency of the free rotational mode known as *Chandler Wobble* (CW)—and to a lesser extent the *Inner Core Wobble* (ICW) (see later). Nutations, on the other hand, are directly affected by the core flow, and so their study offers a window on a broad variety of physical processes taking place inside the fluid core as reviewed in Sect. 4. The fluid core also has an indirect effect on the frequencies of the free rotational modes known as the *Free Core Nutation* (FCN) and *Free Inner Core Nutation* (FICN) that manifest themselves as resonances in the forced nutation series. The FCN also appears in the nutation series at its own free frequency excited by the continual forcing attributed mostly to the atmosphere and oceans. Once deconvolved from the excitation signal, the frequency of this mode provides valuable information about the core (Chao and Hsieh 2015).

Whereas the functional definitions of PM and nutation allow a clear distinction based on the frequencies as stated above, such a distinction does not exist for LOD. ΔLOD contains a broad variety of timescales. In addition to a secular trend, which can be attributed to the luni-solar tidal frictions (Munk and MacDonald 1960) plus contributions from Glacial Isostatic Adjustment (GIA, see later) and tectonic forces (Gross 2015), the total ΔLOD signal contains many oscillations with timescales ranging from decadal, interannual, intra-seasonal, diurnal, and up to subdiurnal. Diurnal and subdiurnal oscillations are attributed to tides (Defraigne and Smits 1999). Oscillations at the interannual, seasonal, and inter-seasonal timescales have been satisfactorily attributed to the exchange of angular momentum between the solid Earth and its fluid envelope (i.e. atmosphere and oceans) (Viron et al. 1999, 2001) while earthquakes have surely induced relatively small changes (see, e.g., Gross and Chao 2006). Although not directly related to rotation, it has been pointed out that the *Slichter modes* with theoretical frequencies of the same order as the subdiurnal PM (as measured in the TRF) might be detectable in the gravimetric signal which calls for caution in interpreting the data (Rosat and Hinderer 2018).

1.4 Implications for the Deep Earth's Dynamics

Of more interest to this review's purpose are the decadal and interannual oscillations in the LOD, the amplitudes of which have been proven too large to be attributed to the atmosphere and oceans solely, thus hinting towards the probable implication of deep interior dynamics, where the core motions are the obvious culprit. In fact, the correlation between the variations in the Earth's magnetic field and the length-of-day variations at decadal timescales (Ball et al. 1969) suggests that the core motions inducing the variations in the magnetic field generate a pressure field at the core–mantle boundary (CMB) causing in turn a change in the Earth's rotation (Hide 1969). Jault et al. (1988) demonstrated that both the frequencies and amplitudes of these ΔLOD fluctuations can be largely explained by the excitation of torsional oscillations, time-variable oscillations in the core flow in the form of coaxial Taylor cylinders around the figure axis which oscillate with a particular period of several years (6 years is typically considered). A more detailed theoretical account of this type of oscillations is given in Triana et al., this issue. The most important implications for our purpose are given in Sect. 3. The existence of the torsional oscillations warrants the close measurement of the decadal ΔLOD.

We thus see how PM, nutations and ΔLOD observations are complementary when examining the nature and dynamics of the flow inside the Earth's core at various timescales. In the remainder of this article, we turn to each of these motions and review the techniques used for their modelling and observations before discussing the fluid core dynamics. Section 5 concludes with perspectives on future work.

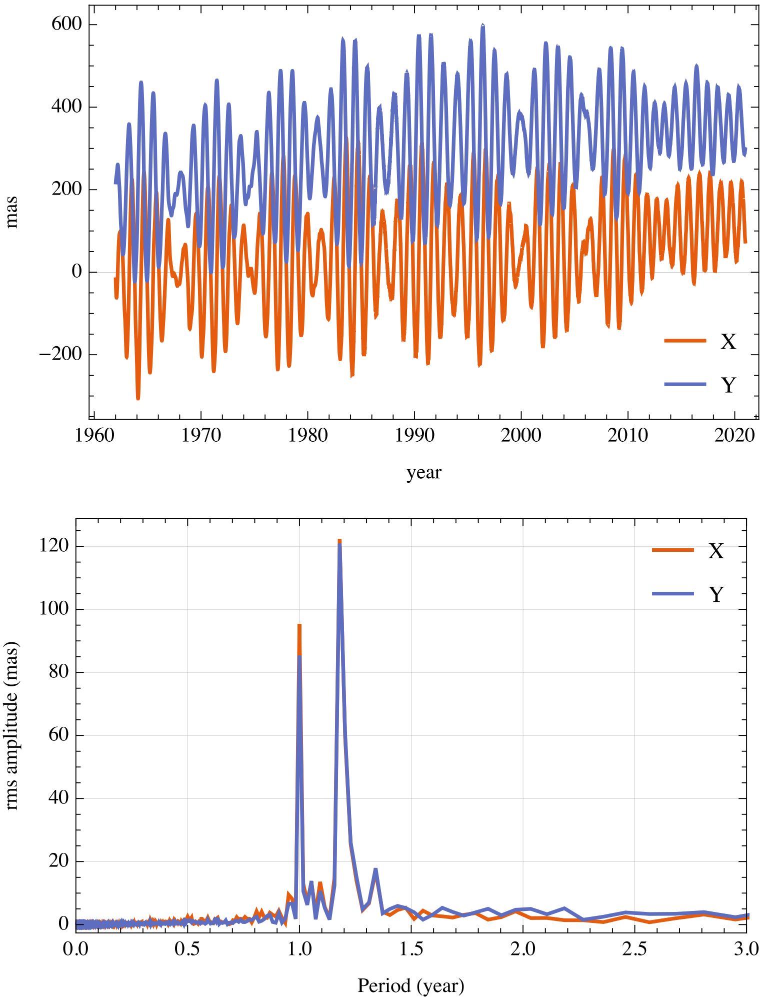

Fig. 2 Polar motion coordinates X and Y, where X is defined towards Greenwich and Y towards 90 degree East as determined by Very Long Baseline Interferometry (VLBI) and Global Navigation Satellite Systems (GNSS) techniques (EOP Combined Serie C04, see details at IERS)

2 Polar Motion

2.1 Modelling and Observations

Polar motion (PM) is the motion of the mean rotation axis (more precisely of the CIP—see Sect. 1) around the symmetry axis of the Earth measured in the TRF. The upper panel of Fig. 2 shows the two components, *X* and *Y*, of this motion for the past six decades based on the EOP Combined Serie C04 (see IERS). The signal has two dominant frequency components, as can be observed from the bottom panel representing its simple Fourier Transform. One of the peaks is at the period of one year, the other corresponds to a period of about 432 days in the TRF. The annual wobble is due to the forcing by surface fluid layers. The

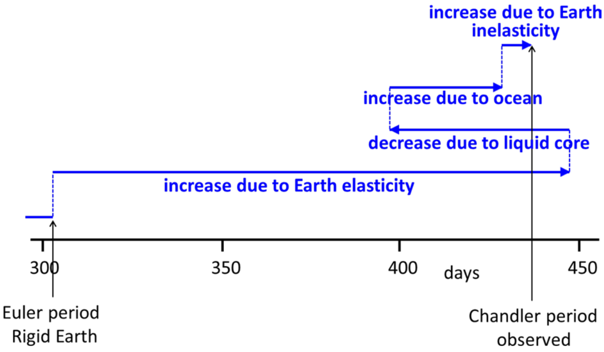

Fig. 3 Period of the CW is altered by a series of geophysical processes

432 days resonance is due to the CW which is the Earth's analog to the *Eulerian nutation* for a rigid ellipsoidal body (Bizouard 2020).

The CW is excited mainly by the atmosphere, the oceans and to a lesser extent by hydrological masses through the afore-mentioned exchange of angular momenta. In practice, geophysical excitation functions are provided by services to the geodesy community (IERS) based on data assimilation and numerical models of the atmosphere and ocean, considering that the oceans are responding dynamically to the atmospheric pressure changes (see, e.g., Bizouard 2020, for details).

The CW is a rotational normal mode whose frequency depends directly on the dynamic oblateness of the Earth modified by the planet's interior structure and feedback from the CW deformation itself (Munk and MacDonald 1960). Mathematically, for an elastic ellipsoidal axisymmetric Earth's model, the CW frequency writes:

$$\sigma_{\mathrm{CW}} = \left(1 - \frac{k_2}{k_s}\right)\sigma_e, \tag{2}$$

where $\sigma_e = \Omega_0(C-A)/A$ is the Eulerian nutation of period 304.5 sidereal days (or 303.6 mean solar days) and $k_2 = 0.302$ and $k_s = 0.942$ are the degree-2 and secular Love numbers that characterize the Earth's elastic and anelastic deformability.

If the oblate Earth were rigid, the period of the CW would be equal to the Eulerian period of $\sim$ 305 sideral days. The Earth having an inelastic mantle, a liquid core, an inelastic inner core, and oceans, this period is in reality about 432 days. These different contributions are shown in Fig. 3, where we see that the presence of a liquid core decreases the CW period by about 40 days. Physically, the CW can be excited by external torques inducing an angle between the principal moment of inertia and the Earth's figure axis or when a large mass redistribution or surface deformation alters the inertia tensor of the Earth, the latter mechanism being the most prominent. The presence of a liquid core changes the mass involved in the mechanism. Mathematically, the CW period will be proportional to the mantle moment of inertia instead of the whole Earth moment of inertia in Eq. (2) when the liquid core does not participate in the motion at the timescale under consideration, reducing the CW period accordingly.

In addition to the CW, the presence of an ellipsoidal inner core introduces another rotational normal mode which can, in principle, become excited when there is a finite angle between the rotation and figure axes of the inner core. This is the ICW introduced in Sect. 1 and is analogous to the CW for the oblate inner core. The moment of inertia of the inner core is 1400 times smaller than the whole Earth's, and its dynamical oblateness is also comparatively smaller. Consequently, the frequency of the ICW is presumably much lower than that of the CW. Additionally, if excited, the ICW would have to transmit its angular momentum to the mantle somehow (e.g., via gravitational torque) in order to observe its contribution to polar motion. So far no firm evidence of the ICW within a resolution of a few mas has been found. A spectral search in PM by Guo et al. (2005) showed that the gravitational perturbation induced by the ICW would be far below the detectability level of current ground (e.g., superconducting gravimeters) and space (e.g., GRACE) gravity measurements. More recently, a 8.7-yr peak detected in PM time-series was suggested to be possibly related to the ICW (Ding et al. 2019), although most of the long-period polar motion, except for the Markowitz period (see below), is generally considered to be attributable to climatological signals.

Beyond the 10-year period, PM is dominated by a 25–35- year pluri-decennal oscillation with a mean amplitude as large as 10 mas. This is the so-called *Markowitz wobble* (Markowitz 1960, 1961). The coupling between core and mantle is believed to be insufficient to explain that term (Hide et al. 1996). As the associated observation errors were too large to definitely conclude about it prior to the use of space geodesy, longer and more precise geodetic time-series should help to further characterize the Markowitz wobble. Centimetre accuracy in the realization of the TRF and of PM is possible thanks to an increasing precision of the space-geodetic observations but necessitates to take into account tectonic plate motions. Considering this and imposing the minimum rotation of the plates as a prepositional condition for the TRF, it is possible to see that the rotation pole has shifted by over 10 meters (about 300 mas) since first defined in 1900. This secular PM is mostly attributed to the *Glacial Isostatic Adjustment* (GIA) modified by present-day ice melting (Adhikari and Ivins 2016) and slightly by large earthquakes (Xu and Chao 2019) in recent years (see below).

In addition to the above-mentioned components, PM signal also contains shorter timescales that correlate with changes in the angular momenta of the atmosphere, ocean and hydrosphere and earthquake. By virtue of the definition of the TRF and CRF evoked in the introduction to this work, the retrograde diurnal motions are equivalent to the wobble associated with nutation. This includes a *Nearly Diurnal Free Wobble* (NDFW) which is perfectly equivalent to the FCN but expressed in the TRF. However, the retrograde diurnal wobble motion is observed as a long-term CIP motion in the CRF including an excitation of the FCN (Bizouard et al. 2019).

2.2 Interpretation

The observed PM is the convolution of the Chandler Wobble resonance with the geophysical excitation function representing Atmospheric, Oceans and Hydrosphere Forcing (AOH) (Munk and MacDonald 1960). The PM excitation function can hence be obtained through a deconvolution procedure (see, e.g., Chao 1985). Its two equatorial components, designated as PM-X and PM-Y, are both characterized by a significant long-term variability on top of strong seasonal and intraseasonal variations (see comparisons in Fig. 4). The seasonal variability in PM-Y is notably larger than that of PM-X. This is attributed to the geographical distribution of major continents which are more aligned in the Y axis and produce relatively larger excitation of PM-Y from atmospheric surface pressure loading and terrestrial water storage changes, whereas atmospheric loading effect over the oceans is largely compensated by the inverted barometer response of the ocean surface. The long-term variability of PM-X and -Y is presumably mainly excited by solid Earth geophysical

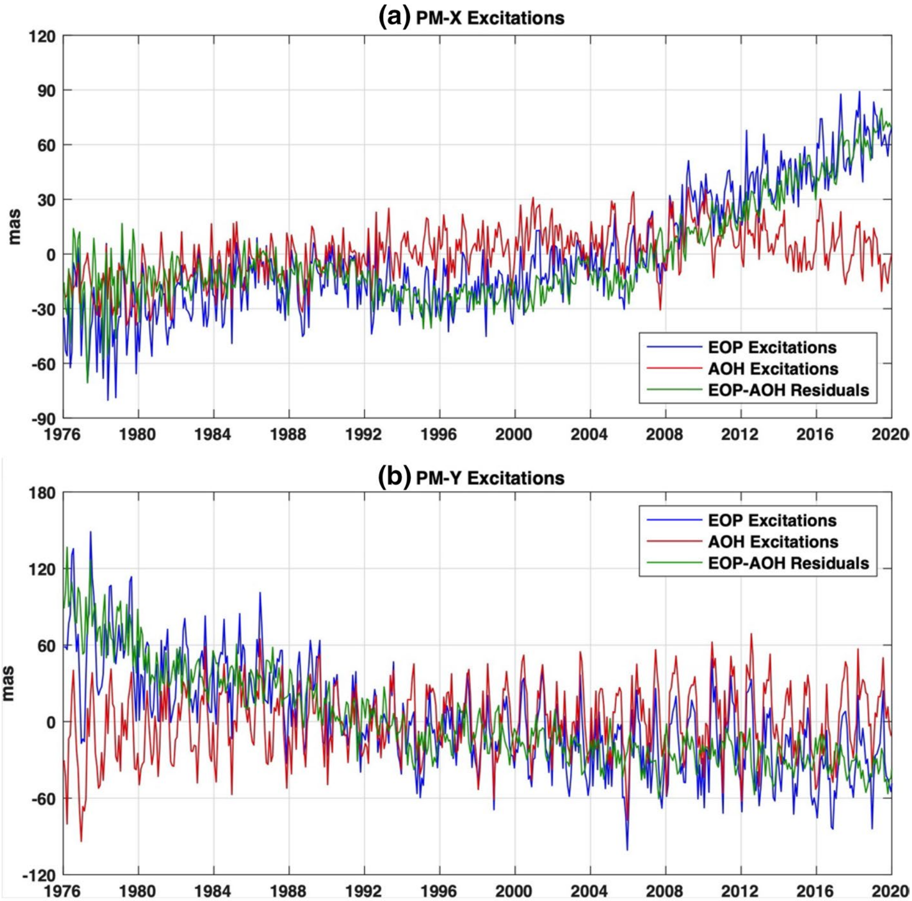

Fig. 4 Deconvolved monthly excitations of the observed polar motion: (**a**) PM-*X* and (**b**) PM-*Y*, from the IERS EOP C04 series and compared geophysical excitations from AOH (the sum of atmospheric, oceanic, and hydrological contributions) over the period 1976–2019. The AOH series are from the GFZ EAM products. EOP-AOH residuals are shown in green curves for comparisons

effects, e.g., GIA (Peltier 2004). At decadal and longer time scales, mass loss in polar ice sheets and glaciers and corresponding sea level changes are found to play a fairly important role in exciting PM as well (Chen et al. 2013; Adhikari and Ivins 2016).

While broad-band decadal variability, other than the Markowitz wobble, is not so evident in PM excitation (as compared to ΔLOD, see Sect. 3), PM-*X* and -*Y* do exhibit clear interannual oscillations. Comprehensive analysis of interannual oscillations in PM excitation and AOH geophysical excitations has been carried out to identify periodic interannual oscillations in both components (Chen et al. 2019). The AOH excitations are from the effective angular momentum (EAM) products provided by the German GeoforschungsZentrum (GFZ) (Dobslaw and Dill 2018). The daily EOP C04 and 3-hourly EAM series have been averaged into monthly intervals. Large uncertainties in EAM series are expected, especially in the hydrological components due to the immaturity of hydrological models. PM-*X* shows a clear oscillation near 5.9 years, plus smaller variations at shorter periods. *Atmospheric, Ocean and Hydrosphere* (AOH) sources largely account for the 2.5–and

3.65–year components found in PM-*Y*. It is interesting to note that AOH excitations also show notable quasi six-year oscillation (SYO) signals in both PM-*X* and -*Y* that are mostly in phase with *Earth's Orientation Parameters* (EOP) Combined Serie C04 (see IERS for details). After AOH excitations are removed, the SYO in PM becomes even less notable so that it is not possible at present to conclude that this SYO in PM, if present, is caused by core processes (Rosat et al. 2020). This is contrary to the case with the SYO in ΔLOD where the SYOs in ΔLOD and AOH are out of phase, and removing AOH makes the SYO in ΔLOD appear more clearly (see Sect. 3).

The quantification of the SYO in PM is more difficult due to the small magnitudes of the signal (compared to seasonal variability) and existence of other interannual oscillations more clearly related to AOH sources. The main challenges in quantifying the SYO in PM, especially the variation related to the solid Earth, include how to improve the quantification of SYO amplitudes and phases in both PM observations and the atmospheric, oceanic and hydrological AOH model predictions. The latter may play a more important role, as the uncertainties of atmospheric, oceanic and hydrological model predictions (including mass and motion terms) appear to be the major limitations affecting the appropriate separation of any SYO signals that might be related to core-mantle interactions (Chen et al. 2019). The magnitudes of the SYO in PM appear to also depend strongly on time spans of the EOP time series. Nevertheless, further investigation of interannual oscillations in PM from both EOP observations and AOH sources is needed.

At multi-decadal time scales, AOH excitations of PM can only be determined from atmospheric, oceanic and hydrological model predictions due to inadequate *in situ* observations. Among the three major components of the climate system, the largest uncertainty appears to come from model-based estimates of terrestrial water storage (TWS) change (Chen and Wilson 2005; Nastula et al. 2019), although it has long been recognized that global TWS change plays an important role in exciting PM at seasonal and interannual time scales (Chen et al. 2000; Nastula et al. 2007).

Another important feature of PM is its attenuation with time due to dissipative processes. Dissipation occurs through anelastic deformation in the mantle, viscomagnetic coupling at the core–mantle boundary, friction at the bottom of the oceans, etc. Dissipation is quantified by a quality factor, *Q*, that may be related to the rheological parameters. The determination of *Q* at the CW frequency, which again requires a Chandler resonance deconvolution, thus provides additional constraints on the Earth rheology at frequencies intermediate between seismic and tidal frequencies (Benjamin et al. 2006).

The movement of the Earth's rotation axis induces a perturbation of the surface gravity field through variation in the centrifugal potential, surface deformation and mass redistribution. These changes have been analysed from superconducting gravimeter (SG) measurements longer than a decade by Ziegler et al. (2016a). In particular, assuming some given rheological models for the Earth's mantle the link between the gravimetric factor phase and the CW quality factor could be made (Ziegler et al. 2016a, b). However, one would need data sets spanning at least 31 years to obtain stable estimates of the CW damping (Gross 2015).

At decadal time-scales, the exchange of angular momentum between the fluid outer core and solid mantle was long thought to be responsible for the observed decadal PM. However, the electro-magnetic (EM) torque computed from geomagnetic observations at the Earth's surface is too weak to explain the observed decadal PM. Notwithstanding, Kuang et al. (2019) have recently simulated the toroidal magnetic field in the D”-layer from the induction and convection of the toroidal field in the outer core showing that it could be much stronger than that from the advection of the poloidal field in the outer core. This reassessment of EM coupling using dynamo simulations shows that it could still contribute largely to decadal PM to magnitude of approximately 10 mas.

Besides CW, measurements of the ICW period would provide a valuable fundamental constraint on the deep Earth's properties. Theoretical estimates based on the conservation of angular momentum and the PREM model of interior predict a period of about 7.5 years prograde. The indirect (resonance) effect of the ICW on nutations hints to a somewhat smaller period of about 2400 days (Mathews et al. 2002b). Ding et al. (2019) have recently showed how the ICW detection could provide a new independent constraint on the density contrast at the ICB. If the detected signal in PM data at 8.7-yr is the signature of the ICW, then it would imply a density contrast of $\sim$ 507 kg/m^3 (Ding et al. 2019). Such a value is smaller than the 600 kg/m^3 for PREM model (see Dehant et al., this issue).

3 ΔLOD

3.1 Modelling and Observations

The best way to measure ΔLOD precisely is by using *Very Long Baseline Interferometry* (VLBI). This technique consists of observing light emitted by radio-sources in S- or X-bands using large antennas on Earth of typically 25 m diameter. The arrival time of the signal at two different stations is then used to compute the (time varying) time delays and infer the Earth orientation relative to the celestial radio-sources taken as stationary (or with a small proper motion characterized *a priori*). After correcting for the time delays induced by atmospheric and other miscellaneous environmental effects, it is possible to derive UT1-UTC, a quantity directly related to the Earth rotation angle with respect to the mean Earth rotation by using a large network of stations and radio-sources (Fey et al. 2015). Information on ΔLOD may then be recovered from:

$$\frac{\Delta \mathrm{LOD}(t)}{\Omega_0} = -\frac{d(\mathrm{UT1} - \mathrm{TAI})}{dt}, \tag{3}$$

where ΔLOD(t) is called the *excess of length of day*, $\Omega_0 = 86400s$ is the mean rotation rate of Earth, UT1 is the Universal Time and TAI is the reference International Atomic Time (related to UTC—Coordinated Universal Time—by a set of leap seconds). VLBI is the only method that can access the absolute UT1 information. It is classically determined weekly by the *International VLBI Service* (IVS) R1 and R4 sessions with an error of the order of $2-3\ \mu s$ (microsecond), as well as via daily one-hour intensive sessions at the level of $\sim 20\ \mu s$ accuracy (Malkin 2020).

ΔLOD takes place on all observable time scales, from subdaily to decadal and beyond (see Fig. 5). It is due to angular momentum changes of the solid Earth in two forms: mass redistribution and the relative motion of the atmosphere, ocean, and the liquid outer core. Tidal forces, primarily from the Sun and Moon, cause ΔLOD through the deformation that they induce on the Earth's mass distribution. These effects are observed using high accuracy space geodetic measurements system (Schuh and Behrend 2012). The periods of the principal zonal tidal components are mostly at the intra-annual timescale with a few notable exception such as the 'regression of the lunar nodes' (*a.k.a.* lunar precession) which has a period of 18.6 years. Table 1 reproduces the 20 tidal components that have the largest effect on ΔLOD (Ray and Erofeeva 2014).

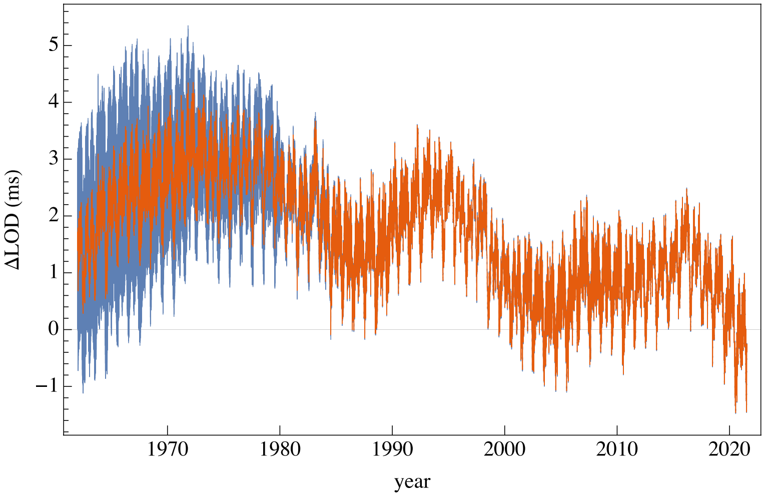

Fig. 5 ΔLOD as measured with VLBI and Global Navigation Satellite Systems (GNSS) techniques (Combined Serie C04, see IERS for details) with uncertainties in blue. ΔLOD contains a rich spectrum of information covering periods from days to multidecadal. It can be partly explained by the mass redistribution or the motion of the atmosphere, the hydrosphere, and the core

The redistribution of masses due to atmospheric, oceanic and hydrological excitations also alter Earth's angular momentum causing ΔLOD at seasonal and interannual timescales. Numerical models computing the angular momentum attributed to meteorological processes have improved significantly in recent years reaching a time resolution of three hours in the evaluation of atmospheric (AAM), oceanic (OAM) and hydrologic (HAM) angular momentum (Dobslaw and Dill 2018). Gross et al. (2004) showed that AAM explains 85.8% of ΔLOD variations at the interannual time scale, but that taking into account OAM and HAM contributions only offers a marginal improvement. In addition, climatic oscillations most likely play a role in ΔLOD. A high correlation was found, for example, between ΔLOD, the El Niño–Southern Oscillation (ENSO) and the quasi-biennial oscillation (Chao 1989).

In addition to the oscillatory components mentioned above, a much longer secular variation is partly attributed to the deceleration caused by tidal frictions in the Earth–Moon system (Munk 1997). The linear regression fitting of ancient ΔLOD observations going back to 4000 years ago based on lunar and solar eclipses records by Babylonian, Chinese, Greek and Arab astronomers predicts a +1.8 ms/cy per century increase in ΔLOD. This is, however, contrasting with the +2.3 ms/cy predicted by tidal friction alone (see Fig. 6) leaving an unexplained gap of about +0.7 ms/cy. Part of this gap is at least partly explicable as the result of the GIA inside the Earth (Mitrovica et al. 2015), a process through which the figure (and the inertia tensor) of the Earth is altered by deglaciation. Models suggest that GIA-induced ΔLOD is very sensitive to the assumed value of lower mantle viscosity (Wu and Peltier 1984; Peltier and Jiang 1996; Peltier 2007) as well as to changes in the mass of glaciers and ice sheets. The Antarctic ice sheet melting-induced mass changes could lead to a −0.72 ms/cy to +0.31 ms/cy in ΔLOD according to Ivins and James (2005). In addition, the subsurface tectonic activities (Van der Wal et al. 2004), earthquakes (Chao and Gross 1987), plate subduction, deformation of the mantle and core–mantle interactions, etc. could

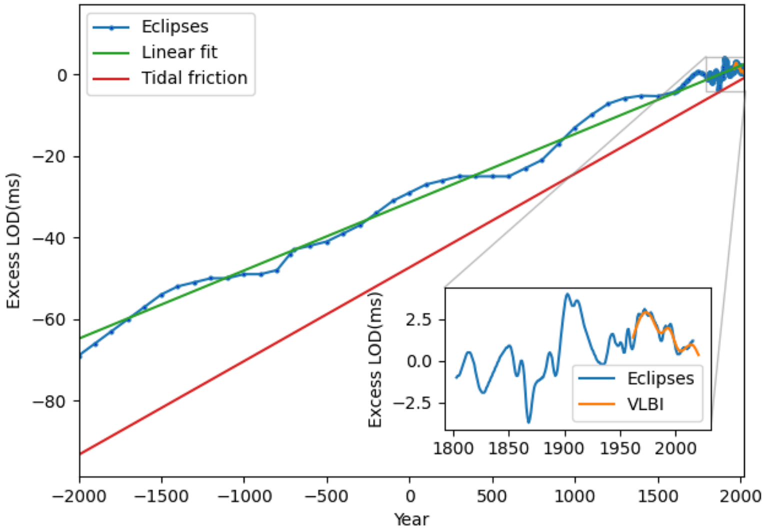

Fig. 6 Secular change in the LOD from 2000 B.C. to present day based on Stephenson et al. (2016). The historical ΔLOD change is estimated from past lunar and solar eclipses documented by Babylonian, Chinese, Greek and Arab astronomers. The linear regression shows a +1.6 ms/cy in ΔLOD with time, which is 0.7 ms/cy lower than the decrease in Earth's rotation rate (+2.3 ms/cy) predicted by tidal friction alone

Table 1 Twenty major zonal tidal components in ΔLOD (reproduced from Ray and Erofeeva (2014))

Period (days)	V_0/g (cm)	UT(cos) (μs)	UT(sin) (μs)	LOD(cos) (μs)	LOD(sin) (μs)
6798.405	2.79288	1764.00	−172958.94	159.851	1.630
3399.202	0.02726	8.46	−840.24	1.553	0.016
1305.483	0.00379	0.47	−44.55	0.214	0.002
1095.178	0.00145	0.15	−14.35	0.082	0.001
385.998	0.00420	0.19	−14.53	0.236	0.003
365.259	0.49215	20.78	−1608.33	27.666	0.358
346.636	0.00311	0.13	−9.64	0.175	0.002
182.621	3.09884	71.94	−5042.06	173.475	2.475
121.749	0.18092	3.20	−195.78	10.104	0.165
31.812	0.67279	6.78	−187.98	37.128	1.339
27.555	3.51840	33.91	−849.42	193.690	7.731
23.942	0.04912	0.45	−10.27	2.696	0.119
14.765	0.58366	4.48	−74.13	31.545	1.908
13.777	0.28836	2.15	−34.07	15.536	0.978
13.661	6.66068	49.36	−779.88	358.699	22.702
9.557	0.24217	1.447	−19.417	12.766	0.952
9.133	1.27531	7.367	−97.403	67.010	5.068
9.121	0.52856	3.050	−40.311	27.770	2.101
7.096	0.20369	0.940	−11.869	10.509	0.832
6.859	0.16872	0.751	−9.480	8.684	0.688

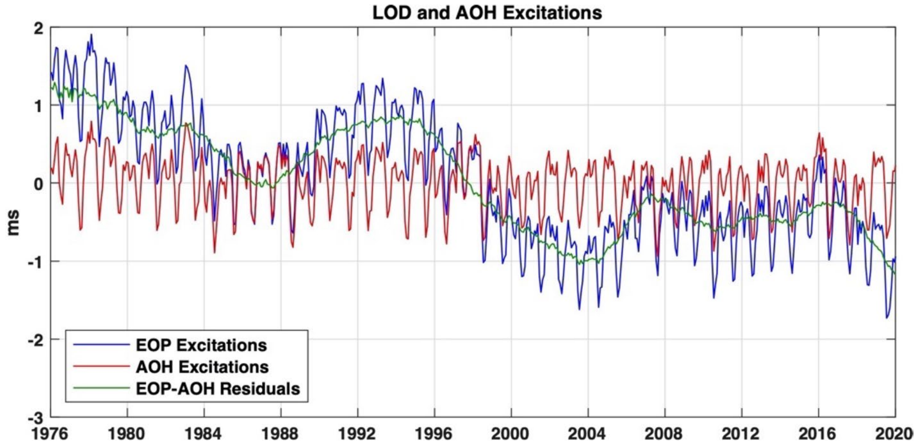

Fig. 7 Comparisons of observed monthly LOD excitations from the IERS EOP C04 series and geophysical excitations from AOH (the sum of atmospheric, oceanic, and hydrological contributions) over the period 1976-2019. The AOH series are from the GFZ EAM products (covering the period 1976 onward)

also alter ΔLOD (Dumberry and Bloxham 2006; Holme 1998; Jault and Le Mouël 1990; Mound and Buffett 2003).

3.2 Interpretation

AAM changes have long been recognized as dominantly driving ΔLOD, accounting for ~ 90% of LOD variations at seasonal and shorter time scales (Rosen and Salstein 1983; Barnes et al. 1983). This is clearly illustrated in the comparisons (shown in Fig. 7) of observed ΔLOD excitations derived from the IERS EOP C04 series and total geophysical excitations from the atmospheric, oceanic, and hydrological contributions (noted as AOH). The strong decadal and long-term variability in LOD is likely driven by mass movement in the interior of Earth and angular momentum exchange between the core and mantle (Jault et al. 1988; Hide et al. 1993; Buffett 1996; Mound and Buffett 2006).

In addition, a quasi-SYO at period of ~ 5.9-year has also been observed in ΔLOD, which could not be attributed to either AAM excitation because of different amplitude and phase (see Fig. 8 and Chen et al. 2019) or to other sources in the surface geophysical fluids system (Abarca del Rio et al. 2000; Chao and Hsieh 2015). Indeed, after removing AOH excitations, the amplitude of the SYO becomes more prominent in the LOD residuals and can be better isolated, as can be seen by comparing the black and red curves in Fig. 8.

This is shown in Fig. 9 showing the time evolution of the LOD power spectrum in the past 4 decades. The SYO indicated by the lower dashed horizontal line is clearly visible.

The remarkable stability of the observed SYO in ΔLOD hints towards a dynamical deep Earth origin (Chao et al. 2014). It is difficult to explain the nearly out of phase SYO in AOH and its dynamical connection with the SYO in observed LOD. It is unlikely to be attributable to errors in the AOH LOD excitations, as similar SYO is also captured in AOH PM excitations, indicating the existence of SYO in the climate system. Further investigations are needed. The quantification of the SYO is also affected by co-existences of other interannual oscillations, in particular a reported 4.9-year (Chen et al. 2019), 8.3-year (Duan and Huang 2020) and 7.3-year (Hsu et al. 2021) oscillation in ΔLOD observations. While

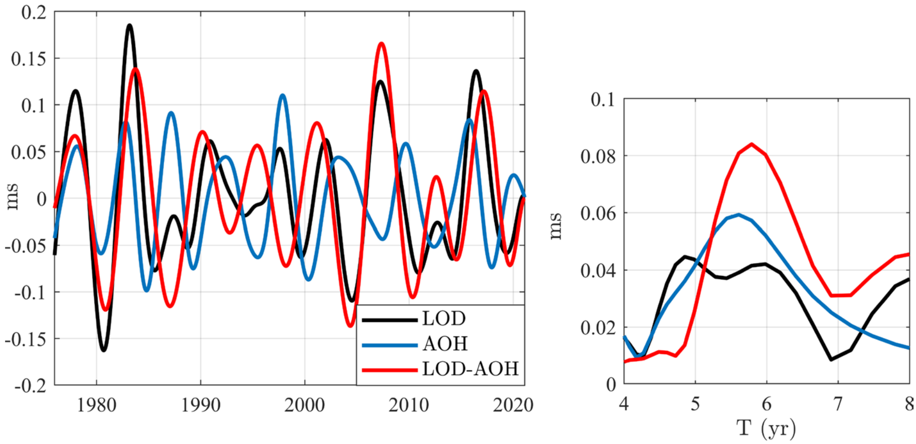

Fig. 8 Observed ΔLOD (only zonal tides were removed), AOH series from the GFZ EAM products and ΔLOD residuals after AOH products were removed. (left) Time-series that were band-pass filtered between 4 and 8 years; (right) amplitude Fourier spectra in ms with respect to period, *T*, in years

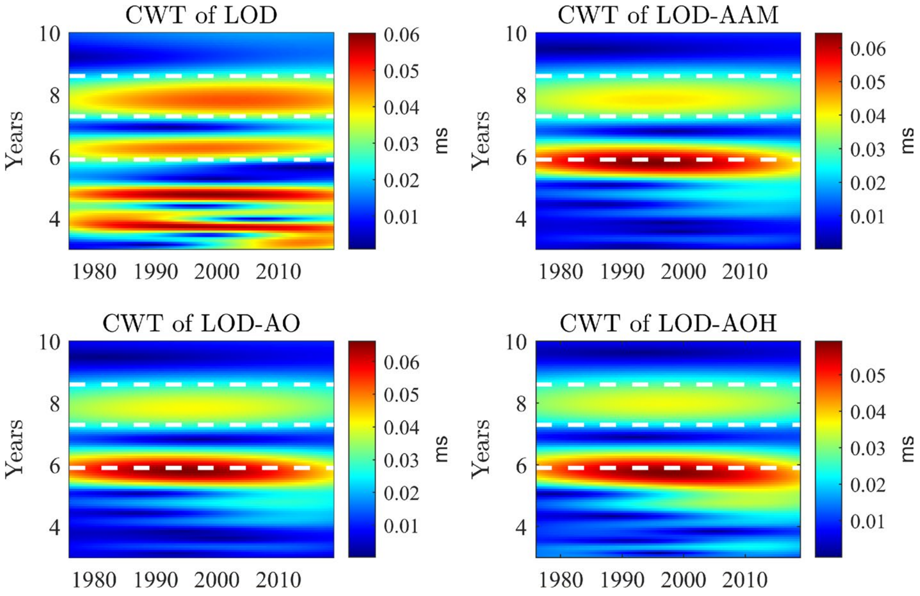

Fig. 9 Continuous Wavelet Transform (CWT) of the LOD signal (upper-left) and the same thing with the contribution from AAM removed (upper-right). Removal of the Oceanic (OAM) and Hydrosphere (HAM) contributions have comparatively small effect on the remaining signal (bottom panels). The horizontal dashed lines correspond to 5.9, 7, and 8.5 years

the 4.9-year oscillation is largely accounted for by AAM (Duan et al. 2015), a possible core origin was suggested for the 8.3 and 7.3-year signals. An extended long record of LOD series is necessary in order to successfully separate these interannual oscillations with close–by periods in ΔLOD (see Fig. 8).

At least two hypotheses have been proposed treating SYO as a rotational normal mode: the Mantle–Inner-Core Gravitational coupling (MICG) (Buffett 1996; Mound and Buffett 2006; Chao 2017; Ding and Chao 2018a; Chao and Yu 2020) and the torsional mode in the fluid outer core (Buffett et al. 2009; Gillet et al. 2010), while certain mechanisms have been postulated for the excitation of the mode (see, e.g., Gillet et al. 2010; Silva et al. 2012; Holme and De Viron 2013). Indeed, the SYO was reported to be correlated with the observed geomagnetic jerks (Bloxham and Jackson 1991) although their remain some open questions and doubt regarding the exact physical nature of this correlation (Ding et al. 2021). Jerks appear at several locations on a time-scale of a few months as sharp V-shaped features in graphs of magnetic field changes (Mandea et al. 2010). A definite physical model is still lacking at the moment to explain their appearance on the global scale. These might be the result of magneto-hydrodynamic waves causing sharp changes in the flow (Aubert and Finlay 2019). Jerks might also be related to the presence of torsional oscillations in the liquid core.

The MICG mechanism, on the other hand, has been the subject of debate because of the amplitude of the strength required to transfer angular momentum between core and mantle through gravitational coupling associated with the inner-core superrotation (Davies et al. 2014). Chao (2017) has further developed the dynamics of the former MICG mechanism in terms of gravitational multipole formulation, in particular for the sectorial quadrupoles of the MICG system that gives rise to the *Axial Torsional Libration* (ATL) of the inner core (see also Chao and Shih 2021). Based on equating the SYO with ATL, postulating that the shape of the inner core conforms to the equipotential surface under the MICG influence, Shih and Chao (2021) deduced separately the equatorial ellipticity of the inner core and the corresponding sectorial quadrupole of the lower mantle plus CMB. The latter has important implications to the density anomaly associated with the constructs of LLSVP (large low shear velocity provinces; see, e.g., McNamara (2019), for a review) residing in the lower mantle above the core-mantle boundary. This constitutes a profoundly interesting case where space-geodesy observed Earth rotation variations serve as key independent information for the inversion of deep Earth structures found in seismological tomography observations. A more detailed discussion of the LLSVP can be found in Dehant et al., this issue.

4 Nutation

4.1 Modelling and Observation

In practice, the conventional initial precession and nutation model is constructed based on a simplified solid Earth model (Kinoshita 1977). The IAU1980 nutation series (Seidelmann 1982) are developed from an elastic rotational oceanless Earth model (Wahr 1981). In those products, the contribution from planetary gravitational attraction was originally neglected. It was introduced around the same time by subsequent works (Roosbeek and Dehant 1998; Bretagnon et al. 1998; Hartmann et al. 1999). All those new series for the rigid Earth were truncated at the level of a tenth of a μas and compared with each others.

Concerning the non-rigid Earth nutations, with the accumulated VLBI observations (see Sect. 3), the discrepancy between observations and the nutation series IAU1980, which were originally quite significant, has been the object of investigation by several authors (Herring et al. 1991). Zhu et al. (1990) developed a method of covariance analysis fitting 106 nutation terms, thereby providing corrections to the IAU1980 series. Herring et al. (2002) later estimated the corrections for 21 major nutation terms with respect to the IAU1980 nutation model and the secular trends in longitude and obliquity with respect to the IAU1977 precession rate from a combined series covering the period from 1980 to 2000. These authors then used the resulting VLBI observation series as input to systematically estimate a series of physical effects such as indirect loading, deformations (estimated through compliances) and the core–mantle coupling constants. They used these parameters (named *Basic Earth Parameters*, see below) to build a non-rigid Earth nutation series named MHB2000. This series was adopted by IAU as the IAU2000 nutation model (Soffel et al. 2003). The correction to the precession rate on the IAU2000 values was discussed by Capitaine et al. (2003), which led to updated IAU2006 precession model, using improved polynomial expressions for the precession. These joint initiatives have led to the new IAU2006/2000A precession-nutation model composed of 678 lunisolar and 687 planetary terms induced by the gravitational attraction from the Moon, the Sun, and the other planets.

Updates and corrections to the major IAU2006/2000A nutation component can be found in Gattano et al. (2017) and Zhu et al. (2021). These authors report an average root-mean-square (RMS) errors after correcting some of the nutation harmonic components of about 130 μas and 110 μas, respectively. Both studies are based on IERS 14C04 EOP observations. Figure 10 (based on Zhu et al. 2021) shows the signal residuals which are mostly dominated by the signature of the FCN.

As discussed in the introduction to this work, the FCN is a free rotational mode with a retrograde frequency as measured from the inertial reference frame. Its excitation results from a misalignment between the rotation axis of the Earth's (spheroidal) liquid outer core and the planet's figure axis (see, e.g., Rekier et al. 2020; Dehant and Mathews 2015). The FCN resonantly amplifies the Earth's response to tidal forcing, as observed in the VLBI data (in the celestial frame) as well as in the retrograde diurnal tidal waves in the records of geophysical sensors in the terrestrial frame (e.g., gravimeters, tiltmeters, strainmeters, etc.); in that latter case, the resonance is designated as the NDFW (see Sect. 2). These resonances have been widely studied by means of VLBI network measurements (Zhu et al. 2021; Herring et al. 1986; Lambert and Dehant 2007; Koot et al. 2008; Rosat and Lambert 2009; Krásná et al. 2013), superconducting gravity records (Florsch and Hinderer 2000; Ducarme et al. 2007; Rosat et al. 2009) or a combination of both (Rosat and Lambert 2009; Ziegler et al. 2020). It is also worth mentioning other experiments performed with strainmeter records (Sato 1991; Zaske et al. 2000; Amoruso et al. 2012; Amoruso and Crescentini 2020) tiltmeters (Riccardi et al. 2018) providing independent, yet somewhat poorer, constraints on the FCN/NDFW parameters. Traces of the FCN are also visible in hydrographic data, demonstrating the observability of the phenomenon long before it was *actually* first observed (Agnew 2018).

The *International VLBI Service* (IVS) is currently working to improve its data through intensive campaigns as well as by developing strategies to balance the current geometry of the VLBI station network. Efforts are also underway in order to incorporate information on the proper motion of distant radio-sources (Lambert 2014). Another source of improvement is provided by the recent reassessment of the influence of atmospheric-oceanic effects on the amplitude of nutations. These have been shown to be particularly important for the prograde annual term (Nurul Huda et al. 2019).

As already mentioned in introduction, in addition to the FCN and FICN resonance effects in the forced nutations, VLBI data feature a contribution from the 'free' FCN mode at the level of a few tenths of mass. The amplitude of this free mode varies with time,

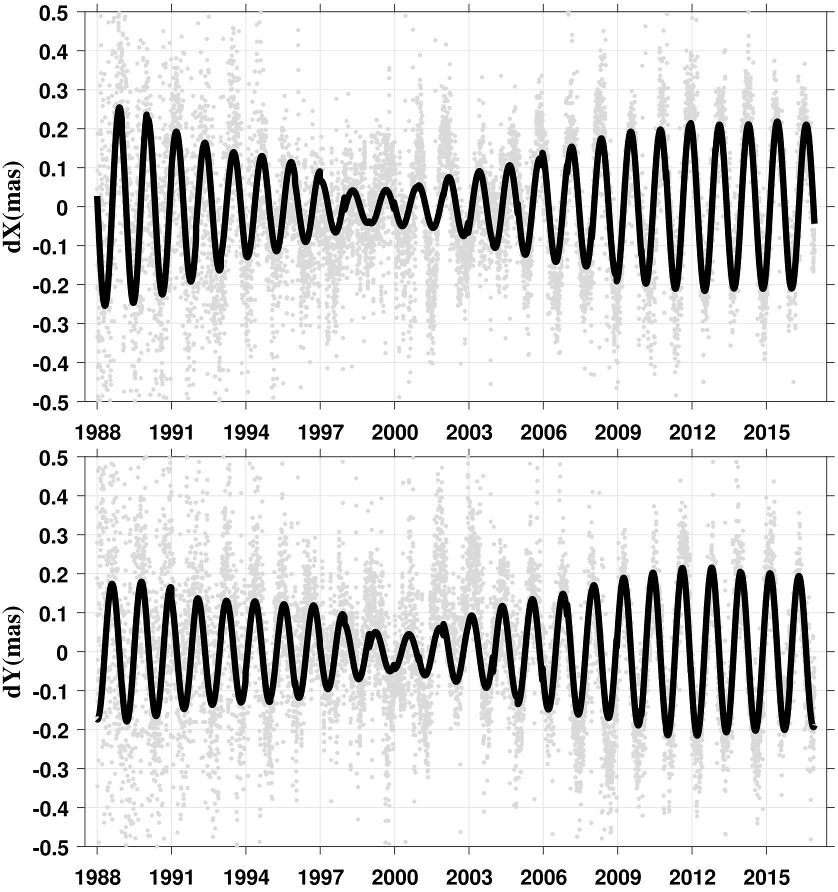

Fig. 10 Nutation residuals from IERS 14C04, which is a combined solution about the IAU2006/IAU2000A precession nutation model. The free core nutation (thick black line) is estimated using an eight years sliding window

which could indicate either a convolution of the free and forced FCN or an interaction between the FCN rotational mode and an inertial mode inside the liquid core (Zhu et al. 2021). Although the existence of this kind of interaction is still largely speculative, it has been demonstrated to be theoretically possible by means of numerical simulations (Triana et al. 2019).

Similar to the FCN, the FICN could, in principle, be observed via its resonance in diurnal tides and nutations, but the effect being small, it has never been clearly detected yet (Rosat et al. 2016). The only constraints obtained on the FICN are via its influence on the long period 18.6-yr nutation term (Mathews et al. 2002a; Koot et al. 2008; Nurul Huda et al. 2019).

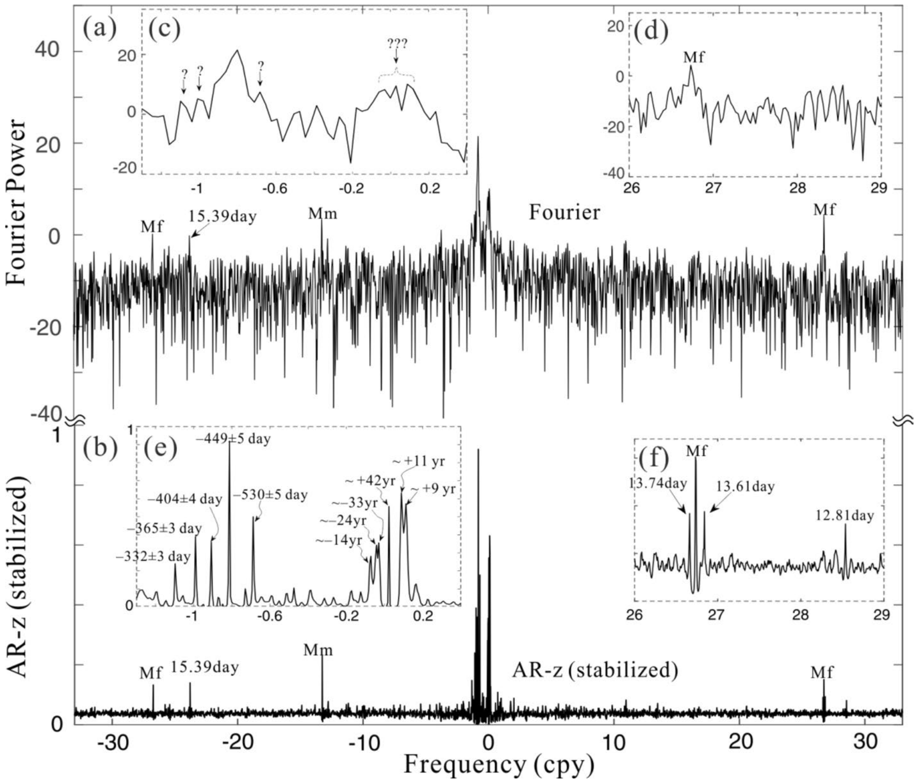

Fig. 11 For the Earth's nutation (1984–2017) in the complex form $\sin\epsilon_0\, d\psi(t) + i\, d\epsilon(t)$ from VLBI data after all the astronomical nutation terms are removed according to model IAU2000A. (**a**) Fourier spectrum (logarithmic scale in dB) and (**b**) stabilized AR-z spectrum. Panels (**c**), (**d**), (**e**), (**f**) and the inset give the zoom-ins of the frequency bands of interest. (taken from Ding and Chao 2018b)

4.2 Interpretations

The nutation series determined from VLBI (see Sect. 4.1) provides the 2-D Earth nutation motion of the CIP relative to the inertial space in terms of the celestial pole offsets $d\psi$ and $d\epsilon$, i.e. the deviations of the longitude ψ and the obliquity ϵ of the equator (relative to $\epsilon_0 = 23.439°$ the mean obliquity of Earth) in the ecliptic coordinates, or often expressed in the complex form $\sin\epsilon_0\, d\psi(t) + i\, d\epsilon(t)$. Or, alternatively, it is simply in terms of the X- and Y-components of the CIP in space.

The free FCN motion is, in principle, the single major signal once all the astronomical nutation terms are removed according to the state-of-the-art nutation model (see, e.g., Zhu et al. 2021) or the reference model values of IAU2000A (Mathews et al. 2002b). The present reference model has a precision of a few mas in the time domain. Only a few nutation components are not properly determined (see Fig. 10). Fitting the amplitudes of these 'new' components allows us to improve the accuracy of the FCN (and FICN) amplification parameters in order to obtain new information about the core.

Figure 11 shows the power spectrum of $\sin\epsilon_0\, d\psi(t) + i\, d\epsilon(t)$, where the positive and negative frequencies correspond to the prograde and retrograde components of the nutational motion in the inertia frame, respectively. Major spectral peaks can be seen in the Fourier spectrum and can be even more distinctively identified in the stabilized AR-z spectrum (Ding and Chao 2018a). At longer periods, Fourier and AR-z nutation spectra show very distinct characteristics (see left portion of the inset of Fig. 11). The Fourier spectrum shows hardly any identifiable peaks other than that corresponding to the FCN, whereas the AR-z spectrum exhibits multiple distinctive peaks, among which only two are readily identifiable: besides the retrograde annual (Sa) nutation as expected, the peak at -449 ± 5 days belongs to the FCN frequency band. It is important to note that the quoted period here is merely FCN's *apparent* value during the timespan covered by the data. It is close to but generally not coinciding with the 'true' natural FCN period because it is a result of convolution of the latter with certain excitation function (Chao and Hsieh 2015). Previous estimates based on a reconstruction from the tide amplified signal give a value within the range of −425 to −435 days for the 'true' FCN. A recent estimate by Zhu et al. (2017) places this value at $T = -429.5 \pm 0.7$ days. Next to the main FCN signal, the presence of secondary spectral peaks of astronomical nutations at tidal periods indicates the imperfection of the reference model IAU2000A. Conversely, these findings provide clues for the reference nutation models.

From what precedes, we see that the FCN is the main window to the structure of the Earth's liquid core as far as nutations are concerned. Comparison between the values of its frequency and quality factor (i.e. its damping) inferred from observation to their theoretical values provides constraints on a number of physical properties. In their simplest form, these properties are represented by a series of parameters describing the strength of the coupling between the solid parts of the Earth (mantle and inner core) and its liquid core. These parameters enter explicitly in the expression of the analytical frequency of the FCN which reads (Mathews et al. 2002b):

$$\frac{\sigma_{\mathrm{FCN}}}{\Omega_0} \simeq -\left(1 + \frac{A_f}{A_m}\right)\left(e_f - \beta + K_{\mathrm{CMB}} + K_{\mathrm{ICB}}\frac{A_s}{A_f}\right), \tag{4}$$

where A_m, A_s and A_f denote the principal axis of inertia of the mantle, solid inner core and fluid outer core, respectively, and e_f is the *dynamical* oblateness of the CMB. Equation (4) is based on the formalism developed by Sasao et al. (1980) in which the values of the two (complex) coupling constants, K_{CMB}, and K_{ICB}, parametrize the total torque that comes in addition to the dynamical pressure torque on the CMB and ICB, respectively (see Dehant et al. 2017). The imaginary parts of K_{CMB} and K_{ICB} represent the damping of the FCN and FICN, related to their quality factor Q, and manifesting itself as a phase lag between the tidal forcing and the induced nutation response. Finally, β is the mantle compliance which accounts for the elastic response of the mantle. This last parameter is typically estimated from interior models, as are A_m, A_s, and A_f. Based on this formalism, Gwinn et al. (1986), and Herring et al. (1986) estimated that the dynamical oblateness of the CMB, e_f, must be $\sim 5\%$ larger than predicted by hydrostatic interior models. This increase, however, cannot account on its own for the whole discrepancy between the observed and derived amplitudes of nutations, nor can it explain the observed phase lag between the tidal forcing and the nutation response (as e_f is a real number, see above). The complete set of so-called *Basic Earth Parameters* (BEP), e_f, K_{CMB} and K_{ICB} (to which one must add the dynamical flattening of the whole Earth, e), can be estimated from data inversion giving the values presented in Table 2 updated from Zhu et al. (2017) (see also Koot et al. 2010).

Three types of contributions to the value of K_{CMB} are generally considered, namely that attributed to the fluid core viscosity, the magnetic field and the topography of the CMB

Table 2 Basic Earth parameters determined from VLBI. The period of the FCN is found equal to $T = -429.5 \pm 0.7$ days (see Zhu et al. 2017, for details)

Parameters	Values	Ranges
$10^3\ e$	3.2845475 ± 7	
$10^3\ (e_f + \mathrm{Re}(K_{\mathrm{CMB}}))$	2.6762 ± 7	[2.67, 2.68]
$10^3\ \mathrm{Im}(K_{\mathrm{CMB}})$	-0.0187 ± 4	[-0.019, -0.018]
$10^3\ \mathrm{Re}(K_{\mathrm{ICB}})$	0.98 ± 3	[0.95, 1.01]
$10^3\ \mathrm{Im}(K_{\mathrm{ICB}})$	-0.92 ± 4	[-0.96, -0.86]

(Buffett et al. 2002; Greff-Lefftz and Legros 1995; Koot and Dumberry 2013). The relative contributions of these torques cannot be easily disentangled, primarily because of the large uncertainty that characterizes the shape and electrical conductivity of the lower mantle. Palmer and Smylie (2005) estimated that the viscous torque caused by the molecular viscosity of the liquid core on the CMB is negligible, being 5 orders of magnitude smaller than the estimates for the electromagnetic (EM) torque. The latter is, however, difficult to model due to our poor knowledge of both the electrical conductivity of the lower part of the mantle as well as the intensity of the non-dipolar part of the magnetic field at this location (whereas the non-dipolar part can be inferred from surface measurements, Langel and Estes 1982; Mathews and Guo 2005). Estimates based on the spectral analysis of the harmonics components of large-scale fields place the rms value of the non-dipolar field at about ~ 0.28mT, the same order of magnitude as the dipolar field. Computations of the EM torque based on this value concluded that the EM torque alone could not explain the values of K_{CMB} and K_{ICB} without assuming a magnetic field amplitude not supported by observations even in the very high conductivity limit (Buffett et al. 2002; Mathews and Guo 2005) and regardless of the shape of the non-dipolar field (Koot and Dumberry 2013). This may point towards the need to reassess the contribution from viscosity upwards by invoking the importance of a larger *effective* viscosity at the CMB (Lumb and Aldridge 1991). This possibility was recently suggested again by Triana et al. (2021) based on their computational estimate of the FCN decay rate due to ohmic and viscous dissipation.

Another ingredient that could potentially complement the effects of the viscous and EM torques is the *topographic torque* produced by the pressure forces within the fluid on a 'rough' CMB. Formally, any deviation of the CMB from an elliptical surface should alter the shape of the flow inside the core, causing it to deviate from the simple solid-body rotation traditionally assumed when modelling the FCN (see Sect. 5). When the amplitude of the CMB topography is small, its effect can be treated as a perturbation. This is the view taken by Wu and Wahr (1997) who predicted a deviation of about 0.2mas on the amplitude of the retrograde annual nutation caused by the small shift in the FCN frequency. However, their results depend strongly on the model of CMB topography chosen. More work is needed to link together the results obtained on the topography with those mentioned above (see also Dehant et al. 2012, on the subject).

Finally, there is the possibility that the FCN might be influenced by the presence of other free modes with nearby frequencies, the natural candidates being *Inertial Modes* of which the FCN is the simplest representative (Rekier et al. 2020; Triana et al. 2021; Rekier et al. 2019). Triana et al. (2019) have shown how these modes can interact in a non-trivial way when the viscosity and ratio of moments of inertia of the core and mantle are such that the FCN frequency and damping are close to that of some other mode thereby causing a shift in the values of the former. Although the regime of parameters at which such interactions can take place is far from that relevant to the Earth, it might theoretically be reachable when the magnetic field is taken into account (Triana et al. 2019).

5 Conclusions and Prospects

Earth's rotation signal covers a broad range of time-scales and contains fundamental information related to deep Earth's processes. The study of these processes is complicated by the influence of surficial processes related to geophysical fluids (i.e. the oceans and atmosphere) that also affect PM, LOD and nutations thus masking smaller core signals. Combined geodetic, magnetic and gravimetric observations have already provided significant constraints on the physics of the outer core boundary. On the other hand, our current knowledge of the inner core is still limited.

Regarding PM and ΔLOD, satellite gravity measurements from GRACE and GRACE Follow-On (GFO) offer a revolutionary means of measuring large-scale mass changes in the climate system, especially those associated with the global hydrological cycle (Tapley et al. 2019), and can help improve the quantification and interpretation of geophysical excitations of ΔLOD and PM (Chen et al. 2016; Göttl et al. 2018; Nastula et al. 2019). GRACE/GFO have collected nearly two decades of time-variable satellite gravity measurements so far, and the series are expected to be extended to well over 20 years (possibly 30). With the future generations of GRACE missions that are under planning, satellite gravimetry will bring a new era of studying geophysical excitations of ΔLOD and PM with unprecedented accuracy. The existence of a 5.9–year variation (SYO) in both PM and ΔLOD signals is intriguing. Although the SYO is almost completely accounted for by surface processes for PM, this is not the case for ΔLOD for which the removal of the AOH contribution only makes the SYO appear more clearly. This hints towards a possible deep interior origin, likely interactions between the core and mantle. In this respect, development of more accurate surficial models (especially in hydrology) and continuous, ever more precise, space observations cannot miss to provide new insights on core processes in the future. As regards the theoretical understanding that this will provide, progress in the near future will most likely come from a better characterization of the interannual oscillations in LOD and PM driven by interactions between the core and mantle. A unified model of these oscillations and how they might relate to core processes that also affect long period nutations (e.g., geomagnetic jerks) is still lacking at the moment and would prove very valuable.

Regarding nutations, continued VLBI observations of nutations will secure the determination of the forced nutation amplitudes in general and the 18.6-year nutation in particular. These nutations are essential to derive the values of the BEP (see Table 2). To be more exact, the BEP allows to determine the imaginary part of the coupling constants, K_{CMB} and K_{ICB}, as well as a combination of the core dynamical flattening, e_f, and the real part of the coupling constant (see Eq. 4). As we already discussed in Sect. 4.2, the relative importance of these parameters cannot be disentangled without making additional hypotheses as regard the nature and dynamics of the flow inside the Earth's core. Therefore, improvement in the current nutation model will necessarily come from a combination of improved measurements and theoretical exploration. The present model currently relies on the following assumptions:

(a) The angular momentum of the liquid core is equal to that of an inviscid non-magnetic and neutrally buoyant flow with uniform vorticity (*a.k.a.* Poincaré flow)

(b) The outer core exchanges angular momentum with the inner core and the mantle via the (dynamic) pressure and electromagnetic torques acting on the ICB and the CMB, both of which approximated as oblate spheroidal surfaces
(c) The damping of the FCN is attributed to the ohmic dissipation inside a thin electrically conducting layer at the base of the mantle

As we already discussed in Sect. 4.2, (a) is well supported by the theoretical study of inertial modes which may be seen as the basis of the fluid motion inside the core (Ivers 2017). However, this simple picture is currently challenged by recent studies that show how angular momentum can be transported through the core when the effects of viscosity, magnetic field and density stratification are taken into account, thereby also questioning both (b) and (c) (see Triana et al., this issue). In the nearest future, progress will most likely come from a detailed reassessment of the viscous and electromagnetic couplings at the CMB. Efforts in this direction are currently undertaken within the GRACEFUL project.

Acknowledgements We would like to extend our gratitude to the anonymous reviewers whose comments helped to significantly improve the quality of our manuscript. The International Space Science Institute (ISSI) is gratefully acknowledged for the support in organizing the workshop that has led to the writing of this paper. The research leading to the results provided by VD, JR and PZ for this paper has received funding from the European Research Council (ERC) under the European Union's Horizon 2020 research and innovation programme (RotaNut Advanced Grant 670874 + GRACEFUL Synergy Grant agreement No 855677).

Declarations

Conflict of interest The authors declare that they have no conflict of interest.

References

Abarca del Rio R, Gambis D, Salstein D (2000) Interannual signals in length of day and atmospheric angular momentum. Ann Geophys 18:347–364

Adhikari S, Ivins ER (2016) Climate-driven polar motion: 2003–2015. Sci Adv 2(4)

Agnew DC (2018) An improbable observation of the diurnal core resonance. Pure Appl Geophys 175(5):1599–1609

Amoruso A, Crescentini L (2020) Parameters of the earth's free core nutation from diurnal strain tides. Sci Rep 10(1)

Amoruso A, Botta V, Crescentini L (2012) Free core resonance parameters from strain data: sensitivity analysis and results from the gran sasso (italy) extensometers. Geophys Jo Int 189(2):923–936

Aubert J, Finlay CC (2019) Geomagnetic jerks and rapid hydromagnetic waves focusing at Earth's core surface. Nat Geosci 12(5):393–398

Ball R, Kahle A, Vestine E (1969) Determination of surface motions of the Earth's core. J Geophys Res 74(14)

Barnes RTH, Hide R, White AA, Wilson CA (1983) Atmospheric angular momentum fluctuations, length-of-day changes and polar motion. Proc Royal Soc London Series A Math Phys Sci 387(1792):31–73

Benjamin D, Wahr J, Ray R, Egbert G, Desai S (2006) Constraints on mantle anelasticity from geodetic observations, and implications for the J2 anomaly. Geophys J Int 165(1):3–16

Bizouard C (2020) Geophysical Modelling of the Polar Motion. De Gruyter, Berlin, Boston

Bizouard C, Nurul Huda I, Ziegler Y, Lambert S (2019) Frequency dependence of the polar motion resonance. Geophys J Int 220(2):753–758

Bloxham J, Jackson A (1991) Fluid flow near the surface of earth's outer core. Rev Geophys 29(1):97–120

Bretagnon P, Francou G, Rocher P, Simon J (1998) Smart97: a new solution for the rotation of the rigid earth. Astron Astrophys 329:329–338

Buffett B, Mathews P, Herring T (2002) Modeling of nutation and precession: effects of electromagnetic coupling. J Geophys Res 107(B4):5.1–5.14:5.1-5.14

Buffett BA (1996) A mechanism for decade fluctuations in the length of day. Geophys Res Lett 23(25):3803–3806

Buffett BA, Mound J, Jackson A (2009) Inversion of torsional oscillations for the structure and dynamics of Earth's core. Geophys J Int 177(3):878–890

Capitaine N, Wallace PT, Chapront J (2003) Expressions for iau 2000 precession quantities. Astron Astrophys 412(2):567–586

Chao B, Hsieh Y (2015) The earth's free core nutation: formulation of dynamics and estimation of eigenperiod from the very-long-baseline interferometry data. Earth Planet Sci Lett 432:483–492

Chao B, Yu Y (2020) Variation of the equatorial moments of inertia associated with a 6-year westward rotary motion in the Earth. Earth Planet Sci Lett 542:116316

Chao BF (1985) On the excitation of the Earth' polar motion. Geophys Res Lett 12(8):526–529

Chao BF (1989) Length-of-day variations caused by el niño-southern oscillation and quasi-biennial oscillation. Science 243(4893):923–925. https://doi.org/10.1126/science.243.4893.923

Chao BF (2017) Dynamics of axial torsional libration under the mantle-inner core gravitational interaction. J Geophys Res Solid Earth 122:560–571

Chao BF, Gross RS (1987) Changes in the earth's rotation and low-degree gravitational field induced by earthquakes. Geophys J Int 91(3):569–596

Chao BF, Shih SA (2021) Multipole expansion: unifying formalism for earth and planetary gravitational dynamics. Surv Geophys. https://doi.org/10.1007/s10712-021-09650-8

Chao BF, Chung W, Shih Z, Hsieh Y (2014) Earth's rotation variations: a wavelet analysis. Terra Nova 26:260–264

Chen J, Wilson CR, Kuang W, Chao BF (2019) Interannual oscillations in Earth Rotation. J Geophys Res Solid Earth 124(12):13404–13414

Chen JL, Wilson CR (2005) Hydrological excitations of polar motion, 1993–2002. Geophys J Int 160(3):833–839

Chen JL, Wilson CR, Chao BF, Shum CK, Tapley BD (2000) Hydrological and oceanic excitations to polar motion andlength-of-day variation. Geophys J Int 141(1):149–156

Chen JL, Wilson CR, Ries JC, Tapley BD (2013) Rapid ice melting drives earth's pole to the east. Geophys Res Lett 40(11):2625–2630

Chen JL, Wilson CR, Ries JC (2016) Broadband assessment of degree-2 gravitational changes from grace and other estimates, 2002–2015. J Geophys Res Solid Earth 121(3):2112–2128

Davies CJ, Stegman DR, Dumberry M (2014) The strength of gravitational core-mantle coupling. Geophys Res Lett 41(11):3786–3792. https://doi.org/10.1002/2014GL059836

de Viron O, Bizouard C, Salstein D, Dehant V (1999) Atmospheric torque on the earth rotation and comparison with atmospheric angular momentum variations. J Geophys Res 104(B3):4861–4875

de Viron O, Ponte R, Dehant V (2001) Atmospheric torque on the earth rotation and comparison with atmospheric angular momentum variations. J Geophys Res 106(B5):8841–8851

Defraigne P, Smits I (1999) Length of day variations due to zonal tides for an inelastic earth in non-hydrostatic equilibrium. Geophys J Int 139(2):563–572

Dehant V, Mathews P (2015) Precession, Nutation, and Wobble of the Earth. Cambridge University Press, Cambridge, p 536

Dehant V, Folgueira M, Puica M (2012) Analytical computation of the effects of the core-mantle boundary topography on tidal length-of-day variations. Proc Journées Systèmes de Référence spatio-temporels 2011, Vianna, Austria pp 113–116

Dehant V, Laguerre R, Rekier J, Rivoldini A, Triana SA, Trinh A, Van Hoolst T, Zhu P (2017) Understanding the effects of the core on the nutation of the Earth. Geodesy Geodyn 8(6):389–395

Ding H, Chao BF (2018a) A 6-year westward rotary motion in the earth: detection and possible MICG coupling mechanism. Earth Planet Sci Lett 495:50–55

Ding H, Chao BF (2018b) Application of stabilized AR-z spectrum in harmonic analysis for geophysics. J Geophys Res: Solid Earth 123:8249–8259. https://doi.org/10.1029/2018JB015890

Ding H, Pan Y, Xu XY, Shen W, Li M (2019) Application of the AR-z spectrum to polar motion: a possible first detection of the inner core wobble and its implications for the density of earth's core. Geophys Res Lett 46(23):13765–13774

Ding H, An Y, Shen W (2021) New evidence for the fluctuation characteristics of intradecadal periodic signals in length-of-day variation. J Geophys Res Solid Earth. https://doi.org/10.1029/2020JB020990

Dobslaw H, Dill R (2018) Predicting earth orientation changes from global forecasts of atmosphere-hydrosphere dynamics. Adv Space Res 61(4):1047–1054

Duan P, Huang C (2020) Intradecadal variations in length of day and their correspondence with geomagnetic jerks. Nat Commun 11:2273. https://doi.org/10.1038/s41467-020-16109-8

Duan P, Liu G, Liu L, Hu X, Hao X, Huang Y, Zhang Z, Wang B (2015) Recovery of the 6-year signal in length of day and its long-term decreasing trend. Earth Planet Space. https://doi.org/10.1186/s40623-015-0328-6

Ducarme B, Sun HP, Xu J (2007) Determination of the free core nutation period from tidal gravity observations of the GGP superconducting gravimeter network. J Geodyn 81:179–187

Dumberry M, Bloxham J (2006) Azimuthal flows in the earth's core and changes in length of day at millennial timescales. Geophys J Int 165(1):32–46

Fey AL, Gordon D, Jacobs CS, Ma C, Gaume RA, Arias EF, Bianco G, Boboltz DA, Böckmann S, Bolotin S, Charlot P, Collioud A, Engelhardt G, Gipson J, Gontier AM, Heinkelmann R, Kurdubov S, Lambert S, Lytvyn S, MacMillan DS, Malkin Z, Nothnagel A, Ojha R, Skurikhina E, Sokolova J, Souchay J, Sovers OJ, Tesmer V, Titov O, Wang G, Zharov V (2015) The second realization of the international celestial reference frame by very long baseline interferometry. The Astron J 150(2):58. https://doi.org/10.1088/0004-6256/150/2/58

Florsch N, Hinderer J (2000) Bayesian estimation of the free core nutation parameters from the analysis of precise tidal gravity data. Phys Earth Planet Inter 117(1):21–35

Gattano C, Lambert SB, Bizouard C (2017) Observation of the earth's nutation by the vlbi: how accurate is the geophysical signal. J Geodesy 91(7):849–856

Gillet N, Jault D, Canet E, Fournier A (2010) Fast torsional waves and strong magnetic field within the Earth's core. Nature 465(7294):74–77

Göttl F, Schmidt M, Seitz F (2018) Mass-related excitation of polar motion: an assessment of the new RL06 GRACE gravity field models. Earth Planet Space 70(1):195

Greff-Lefftz M, Legros H (1995) Core-mantle coupling and polar motion. Phys Earth Planet Inter 91(4):273–283

Gross R (2015) 3.09 - earth rotation variations - long period. In: Schubert G (ed) Treatise on Geophysics (Second Edition), second, edition. Elsevier, Oxford, pp 215–261

Gross RS, Chao BF (2006) The rotational and gravitational signature of the December 26, 2004 Sumatran earthquake. Surv Geophys 27(6):615–632

Gross RS, Fukumori I, Menemenlis D, Gegout P (2004) Atmospheric and oceanic excitation of length-of-day variations during 1980–2000. J Geophys Res Solid Earth 109(B1)

Guo JY, Greiner-Mai H, Ballani L (2005) A spectral search for the inner core wobble in Earth's polar motion. J Geophys Res Solid Earth 110(B10)

Gwinn CR, Herring TA, Shapiro II (1986) Geodesy by radio interferometry: studies of the forced nutations of the Earth: 2. Interpretation. J Geophys Res 91(B5):4755. https://doi.org/10.1029/JB091iB05p04755

Hartmann T, Soffel M, Ron C (1999) The geophysical approach towards the nutation of a rigid earth. Astron Astrophys Suppl Ser 134(2):271–286

Herring T, Mathews P, Buffett B (2002) Modeling of nutation-precession: Very long baseline interferometry results. J Geophys Res Solid Earth 107(B4):ETG–4

Herring TA, Gwinn CR, Shapiro II (1986) Geodesy by radio interferometry: studies of the forced nutations of the Earth: 1. Data analysis. J Geophys Res 91(B5):4745–4754

Herring TA, Buffett BA, Mathews P, Shapiro II (1991) Forced nutations of the earth: influence of inner core dynamics: 3. very long interferometry data analysis. J Geophys Res Solid Earth 96(B5):8259–8273

Hide R (1969) Interaction between the earth's liquid core and solid mantle. Nature 222:599–607

Hide R, Clayton RW, Hager BH, Spieth MA, Voorhdes CV (1993) Topographic Core-Mantle Coupling and Fluctuations in the Earth's Rotation, American Geophysical Union (AGU), pp 107–120

Hide R, Boggs DH, Dickey JO, Dong D, Gross RS, Jackson A (1996) Topographic core-mantle coupling and polar motion on decadal time-scales. Geophys J Int 125(2):599–607

Holme R (1998) Electromagnetic core-mantle coupling-i. explaining decadal changes in the length of day. Geophys J Int 132(1):167–180

Holme R, De Viron O (2013) Characterization and implications of intradecadal variations in length of day. Nature 499:202–204

Hsu CC, Duan PS, Xu XQ, Zhou YH, Huang CL (2021) On the ~7 year periodic signal in length of day from a frequency domain stepwise regression method. J Geodesy 95:55. https://doi.org/10.1007/s00190-021-01503-x

Ivers D (2017) Enumeration, orthogonality and completeness of the incompressible Coriolis modes in a tri-axial ellipsoid. Geophys Astrophys Fluid Dyn 111(5):333–354. https://doi.org/10.1080/03091929.2017.1330412

Ivins ER, James TS (2005) Antarctic glacial isostatic adjustment: a new assessment. Antarctic Sci 17(4):541

Jault D, Le Mouël JL (1990) Core-mantle boundary shape: constraints inferred from the pressure torque acting between the core and the mantle. Geophys J Int 101(1):233–241

Jault D, Gire C, Le Mouel JL (1988) Westward drift, core motions and exchanges of angular momentum between core and mantle. Nature 333(6171):353–356

Kinoshita H (1977) Theory of the rotation of the rigid earth. Celes Mech 15(3):277–326

Koot L, Dumberry M (2013) The role of the magnetic field morphology on the electromagnetic coupling for nutations. Geophys J Int 195(1):200–210

Koot L, Rivoldini A, de Viron O, Dehant V (2008) Estimation of earth interior parameters from a Bayesian inversion of very long baseline interferometry nutation time series. J Geophys Res 113(B08414)

Koot L, Dumberry M, Rivoldini A, de Viron O, Dehant V (2010) Constraints on the coupling at the core-mantle and inner core boundaries inferred from nutation observations. Geophys J Int 182:1279–1294

Krásná H, Böhm J, Schuh H (2013) Free core nutation observed by VLBI. Astronon Astrophys 555:29

Kuang W, Chao BF, Chen J (2019) Reassessment of electromagnetic core-mantle coupling and its implications to the Earth's decadal polar motion. Geodesy Geodyn 10(5):356–362

Lambert SB (2014) Comparison of VLBI radio source catalogs. Astron Astrophys 570:108

Lambert SB, Dehant V (2007) The Earth's core parameters as seen by the VLBI. Astronon Astrophys 469:777–781

Langel RA, Estes RH (1982) A geomagnetic field spectrum. Geophys Res Lett 9(4):250–253. https://doi.org/10.1029/GL009i004p00250

Lumb LI, Aldridge KD (1991) On viscosity estimates for the Earth's fluid outer core and core-mantle coupling. J Geomag Geoelectr 43(2):93–110. https://doi.org/10.5636/jgg.43.93

Malkin ZM (2020) Statistical analysis of the results of 20 years of activity of the international VLBI service for geodesy and astrometry. Astron Rep 64(2):168–188

Mandea M, Holme R, Pais A, Pinheiro K, Jackson A, Verbanac G (2010) Geomagnetic jerks: rapid core field variations and core dynamics. Space Sci Rev 155(1–4):147–175

Markowitz W (1960) Latitude and longitude, and the secular motion of the pole. Methods Tech Geophys pp 325–361

Markowitz W (1961) International determination of the total motion of the pole. Bul Geod 59:29–41

Mathews P, Herring TA, Buffett BA (2002a) Modeling of nutation precession: new nutation series for non-rigid Earth and insights into the Earth's interior. J Geophys Res 107(B4):ETG3–1–3–30

Mathews PM, Bretagnon P (2003) Polar motions equivalent to high frequency nutations for a nonrigid Earth with anelastic mantle. Astron Astrophys 400(3):1113–1128. https://doi.org/10.1051/0004-6361:20021795

Mathews PM, Guo JY (2005) Viscoelectromagnetic coupling in precession-nutation theory. J Geophys Res Solid Earth. 10.1029/2003JB002915

Mathews PM, Herring TA, Buffett BA (2002b) Modeling of nutation and precession: new nutation series for nonrigid earth and insights into the earth's interior. J Geophys Res Solid Earth. 10.1029/2001JB000390

McNamara AK (2019) A review of large low shear velocity provinces and ultra low velocity zones. Tectonophysics 760:199–220

Mitrovica JX, Hay CC, Morrow E, Kopp RE, Dumberry M, Stanley S (2015) Reconciling past changes in Earth's rotation with 20th century global sea-level rise: resolving Munk's enigma. Sci Adv 1(11):e1500679. https://doi.org/10.1126/sciadv.1500679

Mound J, Buffett B (2003) Interannual oscillations in length of day: Implications for the structure of the mantle and core. J Geophys Res Solid Earth 108(B7)

Mound JE, Buffett BA (2006) Detection of a gravitational oscillation in length-of-day. Earth Planet Sci Lett 243(3):383–389

Munk W (1997) Once again: once again-tidal friction. Prog Oceanogr 40(1–4):7–35

Munk W, MacDonald G (1960) The Rotation of the Earth: a Geophysical Discussion. Cambridge Univ Press, Cambridge

Nastula J, Ponte RM, Salstein DA (2007) Comparison of polar motion excitation series derived from grace and from analyses of geophysical fluids. Geophys Res Lett 34(11)

Nastula J, Wińska M, Śliwińska J, Salstein D (2019) Hydrological signals in polar motion excitation - evidence after fifteen years of the grace mission. J Geodyn 124:119–132

Nurul Huda I, Lambert S, Bizouard C, Ziegler Y (2019) Nutation terms adjustment to vlbi and implication for the earth rotation resonance parameters. Geophys J Int 220(2):759–767

Palmer A, Smylie D (2005) Vlbi observations of free core nutations and viscosity at the top of the core. Phys Earth Planet Inter 148(2):285–301. https://doi.org/10.1016/j.pepi.2004.09.003

Peltier W (2004) Global glacial isostasy and the surface of the ice-age earth: the ice-5g (vm2) model and grace. Ann Rev Earth Planet Sci 32(1):111–149

Peltier W (2007) History of earth rotation. Treatise Geophys 9:243–293

Peltier W, Jiang X (1996) Glacial isostatic adjustment and earth rotation: refined constraints on the viscosity of the deepest mantle. J Geophys Res Solid Earth 101(B2):3269–3290

Ray RD, Erofeeva SY (2014) Long-period tidal variations in the length of day. J Geophys Res Solid Earth 119(2):1498–1509

Rekier J, Trinh A, Triana SA, Dehant V (2019) Inertial modes in near-spherical geometries. Geophys J Int 216(2):777–793. https://doi.org/10.1093/gji/ggy465

Rekier J, Triana SA, Trinh A, Dehant V (2020) Inertial modes of a freely rotating ellipsoidal planet and their relation to nutations. Planet Sci J 1(1):20

Riccardi U, Boy JP, Hinderer J, Rosat S, Boudin F (2018) Free Core Nutation Parameters from Hydrostatic Long-Base Tiltmeter Records in Sainte Croix aux Mines (France). In: Freymueller, JT and Sanchez, L (ed) International Symposium on Earth and Environmental Sciences for Future Generations, International Association of Geodesy Symposia, vol 147, pp 171–179

Roosbeek F, Dehant V (1998) Rdan97: an analytical development of rigid earth nutation series using the torque approach. Celes Mech Dyn Astron 70(4):215–253

Rosat S, Hinderer J (2018) Limits of Detection of Gravimetric Signals on Earth. Sci Rep 8(1):15324. https://doi.org/10.1038/s41598-018-33717-z

Rosat S, Lambert SB (2009) Free core nutation resonance parameters from VLBI and superconducting gravimeter data. Astron Astrophys 503:287–291

Rosat S, Florsch N, Hinderer J, Llubes M (2009) Estimation of the free core nutation parameters from SG data: sensitivity study and comparative analysis using linearized Least-Squares and Bayesian methods. J Geodyn 48:331–339

Rosat S, Calvo M, Lambert S (2016) Detailed Analysis of Diurnal Tides and Associated Space Nutation in the Search of the Free Inner Core Nutation Resonance. In: Freymueller J, Sánchez L (eds) International Symposium on Earth and Environmental Sciences for Future Generations, Springer, International Association of Geodesy Symposia, vol 147

Rosat S, Gillet N, Boy JP, Couhert A, Dumberry M (2020) Interannual variations of degree 2 from geodetic observations and surface processes. Geophys J Int. 10.1093/gji/ggaa590

Rosen RD, Salstein DA (1983) Variations in atmospheric angular momentum on global and regional scales and the length of day. J Geophys Res Oceans 88(C9):5451–5470

Sasao T, Okubo S, Saito M (1980) A Simple Theory on the Dynamical Effects of a Stratified Fluid Core upon Nutational Motion of the Earth. Springer, Netherlands, Dordrecht, pp 165–183

Sato T (1991) Fluid core resonance measured by quartz tube extensometers at Esashi earth tide station. In: Kakkuri J (ed) Proceedings of the 11th International Symposium on Earth tides, pp 573–582

Schuh H, Behrend D (2012) Vlbi: a fascinating technique for geodesy and astrometry. J Geodyn 61:68–80

Seidelmann P (1982) 1980 iau theory of nutation: the final report of the iau working group on nutation. Celes Mech 27(1):79–106

Shih SA, Chao BF (2021) Inner core and its libration under gravitational equilibrium: implications to lower-mantle density anomaly. J Geophys Res Solid Earth, 10.1029/2020JB020541

Silva L, Jackson L, Mound J (2012) Assessing the importance and expression of the 6 year geomagnetic oscillation. J Geophys Res Solid Earth 117(B10)

Soffel M, Klioner SA, Petit G, Wolf P, Kopeikin S, Bretagnon P, Brumberg V, Capitaine N, Damour T, Fukushima T et al (2003) The iau 2000 resolutions for astrometry, celestial mechanics, and metrology in the relativistic framework: explanatory supplement. The Astron J 126(6):2687

Stephenson F, Morrison L, Hohenkerk C (2016) Measurement of the earth's rotation: 720 bc to ad 2015. In: Proceedings of the Royal Society A: Mathematical, Physical and Engineering Sciences 472(2196):20160404

Tapley BD, Watkins MM, Flechtner F, Reigber C, Bettadpur S, Rodell M, Sasgen I, Famiglietti JS, Landerer FW, Chambers DP, Reager JT, Gardner AS, Save H, Ivins ER, Swenson SC, Boening C, Dahle C, Wiese DN, Dobslaw H, Tamisiea ME, Velicogna I (2019) Contributions of GRACE to understanding climate change. Nat Clim Change 9(5):358–369

Triana S, Rekier J, Trinh A, Dehant V (2019) The coupling between inertial and rotational eigenmodes in planets with liquid cores. Geophys J Int 218:375–389

Triana SA, Trinh A, Rekier J, Zhu P, Dehant V (2021) The viscous and ohmic damping of the earth's free core nutation. J Geophys Res Solid Earth 126(4):1–14

Wahr JM (1981) The forced nutations of an elliptical, rotating, elastic and oceanless earth. Geophys J Int 64(3):705–727

Van der Wal W, Schotman H, Vermeersen L (2004) Geoid heights due to a crustal low viscosity zone in glacial isostatic adjustment modeling: a sensitivity analysis for goce. Geophys Res Lett 31(5)

Wu P, Peltier W (1984) Pleistocene deglaciation and the earth's rotation: a new analysis. Geophys J Int 76(3):753–791

Wu X, Wahr J (1997) Effects of non-hydrostatic core-mantle boundary topography and core dynamics on earth rotation. Geophys J Int 128:18–42

Xu CY, Chao BF (2019) Seismic effects on the secular drift of the earth's rotational pole. J Geophys Res Solid Earth 124(6):6092–6100. https://doi.org/10.1029/2018JB017164

Zaske J, Zürn W, Wilhelm H (2000) NDFW analysis of Borehole water level data from the hot-dry-rock test site soultz-sous-forêts. Bull d'Information des Marées Terrestres 132:10241–10270

Zhu P, Rivoldini A, Koot L, Dehant V (2017) Basic earth's parameters as estimated from vlbi observations. Geodesy Geodyn 8(6):427–432

Zhu P, Triana SA, Rekier J, Trinh A, Dehant V (2021) Quantification of corrections for the main lunisolar nutation components and analysis of the free core nutation from vlbi observed nutation residuals. J Geodesy. https://doi.org/10.1007/s00190-021-01513-9

Zhu S, Groten E, Reigber C (1990) Various aspects of numerical determination of nutation constants. ii-an improved nutation series for the deformable earth. The Astron J 99:1024–1044

Ziegler Y, Hinderer J, Rogister Y, Rosat S (2016a) Estimation of the gravimetric pole tide by stacking long time-series of GGP superconducting gravimeters. Geophys J Int 205(1):77–88

Ziegler Y, Rogister Y, Hinderer J, Rosat S (2016b) Chandler Wobble and Frequency Dependency of the Ratio Between Gravity Variation and Vertical Displacement for a Simple Earth Model with Maxwell or Burgers Rheologies. In: JT F, L S (eds) International Symposium on Earth and Environmental Sciences for Future Generations, Springer, International Association of Geodesy Symposia, vol 147

Ziegler Y, Lambert SB, Huda IN, Bizouard C, Rosat S (2020) Contribution of a joint Bayesian inversion of VLBI and gravimetric data to the estimation of the free inner core nutation and free core nutation resonance parameters. Geophys J Int 222(2):845–860